SAND--98-8450C

Some Chemical Kinetics Issues in Reburning: The Branching Fraction of the HCCO + NO Reaction

CONF-980804--

James A. Miller and Joseph L. Durant
Combustion Research Facility
Sandia National Laboratories
Livermore, CA 94551-0969, U.S.A.
and
Peter Glarborg
Department of Chemical Engineering
Technical University of Denmark
2800 Lyngby, Denmark

Corresponding Author: James A. Miller
e-mail: jamille@ca.sandia.gov
or
jim@jamndgo.ca.sandia.gov

FAX: (510) 294-2276
Phone: (510) 294-2759

Word Count:

10 pages of text and references @ 350 words/page	3,500
5 figures @ 200 words each	1,000
1 table @ 200 words	200
TOTAL	4,700 Words

DISCLAIMER

Some Chemical Kinetics Issues in Reburning: The Branching Fraction of the HCCO + NO Reaction

James A. Miller and Joseph L. Durant
Combustion Research Facility
Sandia National Laboratories
Livermore, CA 94551-0969, U.S.A.
and
Peter Glarborg
Department of Chemical Engineering
Technical University of Denmark
2800 Lyngby, Denmark

ABSTRACT

We have determined theoretically some critical kinetic parameters in the mechanism of NO_x reburning under flow-reactor conditions. Specifically, using a variety of electronic-structure methods to investigate the potential energy surfaces and the maximum free energy method of Quack and Troe to determine the resulting rate coefficients, we have deduced the values of k_2 and k_3 for the reactions,

$$HCNO + O \leftrightarrow HCO + NO \quad (R2)$$

and

$$HCNO + OH \leftrightarrow HCOH + NO, \quad (R3)$$

to be $k_2 \approx 7 \times 10^{13}$ cm^3/mole-sec. and $k_3 \approx 2 \times 10^{13}$ cm^3/mole-sec. independent of temperature for 300 K < T < 2700 K. With such fast reactions converting HCNO to NO, a critical parameter in the reburn mechanism is $\alpha(T) = k_{1b}(T)/k_1(T)$, the branching fraction of the HCCO + NO reaction,

$$HCCO + NO \leftrightarrow HCNO + CO \quad (R1a)$$
$$\leftrightarrow HCN + CO_2 \quad (R1b)$$
$$\leftrightarrow HONC + CO. \quad (R1c)$$

Again using PES information from a variety of electronic-structure methods, we have used the statistical-theoretical methodology of Miller, Parrish, and Brown to determine $\alpha(T) = 0.985 \exp(-T/1748)$, valid for 300 K < T < 2000 K. Using a value of $k_1 = k_{1a} + k_{1b} + k_{1c} = 2.4 \times 10^{13}$ cm^3/mole-sec. independent of temperature (consistent with experiment) we have determined modified Arrhenius expressions for k_{1a} and k_{1b}, $k_{1a} = 1.17 \times 10^{13}\ T^{0.65}$ cm^3/mole-sec. and $k_{1b} = 1.45 \times 10^{16}\ T^{-0.968} \exp(-648/RT)$ cm^3/mole-sec for 300 K < T < 2000 K. Reaction (R1c) never contributes as much as 1% to the total rate coefficient.

The theoretical analyses and the reburn mechanism are discussed in detail.

I. Introduction

Reburning [1-3] is a potentially powerful tool for controlling NO_x emissions from combustion sources [4, 5]. It was developed for use on stationary power plants, particularly coal-fired boilers and furnaces. In the "reburn mode," fuel is burned in three separate stages. Most of the fuel (approximately 85%) is consumed in the first stage, which is operated under slightly lean to stoichiometric conditions. It is this primary stage that produces the NO, as well as other combustion products. In the second stage a cleaner fuel, usually natural gas, is injected into the products of the first stage, creating a fuel-rich "reburn" zone, where small hydrocarbon free radicals react with the NO, converting it primarily to molecular nitrogen and hydrogen cyanine [6-8]. Additional air is introduced in the third stage in order to complete the oxidation of any hydrocarbons and CO left from the second stage. In this burnout zone the hydrogen cyanide from the second stage may be either oxidized to NO or converted to N_2. In either case the overall three-stage process results in considerably lower NO_x emissions than if the fuel were burned in a single stage.

Understanding the chemistry of the reburn zone is clearly a key to understanding and optimizing reburn technology. Recently a number of papers have appeared [e.g. 4, 5, 9, 10] that attempt to characterize this chemistry in some detail, either through chemical kinetic modeling, flow-reactor experiments, or a combination of the two. A particularly stimulating paper is that due to Stapf and Leuckel [9]. These authors studied the reaction of natural gas with NO in a laboratory-scale plug-flow reactor at temperatures of 1473 K, 1573 K, and 1673 K and at equivalence ratios from ϕ= 1.1 to ϕ = 1.6. They find that the reaction mechanisms of Miller and Bowman [6], Glarborg and Hadvig [11], and Bockhorn, et al [12] are not able to account quantitatively for their experimental results. All three mechanisms overestimate the NO removal and the HCN production, particularly under high oxygen concentrations. In all three mechanisms the critical NO removal step is the reaction between ketenyl and nitric oxide,

$$HCCO + NO \leftrightarrow HCNO + CO, \qquad \text{(R1a)}$$

a reaction first hypothesized by Miller and Bowman [6]. In order to remedy the situation, Stapf and Leuckel adopted a model in which reaction (R1a) was suppressed, and the rate coefficients for the two-channel reaction,

$$CH_3 + NO \leftrightarrow HCN + H_2O \qquad \text{(R4a)}$$
$$\leftrightarrow H_2CN + OH, \qquad \text{(R4b)}$$

were increased to the values obtained experimentally by Braun-Unkhoff et al [13]. Such a model was able to account satisfactorily for their experimental results.

The rate coefficient for reaction (R1),

$$HCCO + NO \leftrightarrow HCNO + CO \qquad \text{(R1a)}$$
$$\leftrightarrow HCN + CO_2 \qquad \text{(R1b)}$$

is now reasonably well established experimentally [14-16], at least up to a temperature of approximately 700 K. The experimental results are consistent with a temperature-independent rate coefficient, $k_1 = 2.4 \times 10^{13}$ cm^3/mole-sec., which is not much smaller than the Miller-

Bowman estimate of $k_1 = 3.0 \times 10^{13}$ cm^3/mole-sec. Therefore, one must conclude that suppressing (R1) in kinetic models is not a reasonable alternative.

We have recently been involved in modeling a wide range (i.e. different fuels, equivalence ratios, levels of dilution, etc.) of flow reactor experiments to gain insight into the reburn mechanism under flow-reactor conditions [17, 18]. In the mechanism we have adopted, NO removal is dominated by the HCCO + NO reaction,

$$\text{HCCO} + \text{NO} \leftrightarrow \text{HCNO} + \text{CO} \qquad \text{(R1a)}$$
$$\leftrightarrow \text{HCN} + \text{CO}_2 \qquad \text{(R1b)}$$

with only a secondary contribution from the CH_3 + NO reaction, even when methane is the fuel. There are two critical issues in our mechanism. First, in order to account at least qualitatively for the observations of Stapf and Leuckel, we have included fast reactions of HCNO with OH and O,

$$\text{HCNO} + \text{O} \leftrightarrow \text{HCO} + \text{NO} \qquad \text{(R2)}$$
$$+ \text{OH} \leftrightarrow \text{HCOH (or } \text{CH}_2\text{O}) + \text{NO.} \qquad \text{(R3)}$$

This has the effect of making reaction (R1a) ineffective in removing NO, because the NO removed by (R1a) is simply reformed through (R2) and (R3). Second, when such fast reactions are included in the mechanism, the branching fraction $\alpha(T)$ of the HCCO + NO reaction, $\alpha(T) = k_{1b}(T)/k_1(T)$, becomes a critical parameter in the modeling, because it determines the extent to which NO is converted to hydrogen cyanide. In our mechanism we have taken $\alpha(T) \approx 0.65$, the same as that determined experimentally (and theoretically) [19, 20] for the isoelectronic NCO + NO reaction. Such a value gives generally good agreement between model and experiment.

The purpose of the present paper is to investigate theoretically the feasibility of the mechanism described in the previous paragraph. Such theory has become a powerful tool in gaining insight into combustion chemistry [21].

II. The Reburn Mechanism

It is important to understand how the free radicals responsible for NO removal in reburning are formed during fuel oxidation under flow reactor conditions. To this end we have included Fig. 1, which is a reaction-path diagram (following the fuel carbon) drawn from the modeling of Prada and Miller [18] and Glarborg, et al. [17]. The diagram is not intended to be exhaustive, but only to show how HCCO and CH_3, the free radicals primarily responsible for the conversion of NO to HCN, arise during the reburning process.

If ethane is the reburn fuel, the primary path to ketenyl is as follows:

$$\text{C}_2\text{H}_6 + \text{OH (H)} \rightarrow \text{C}_2\text{H}_5 + \text{H}_2\text{O (H}_2\text{)} \qquad \text{(R5)}$$
$$\text{C}_2\text{H}_5 \text{ (+M)} \rightarrow \text{C}_2\text{H}_4 + \text{H (+M)} \qquad \text{(R6)}$$
$$\text{C}_2\text{H}_4 + \text{OH (H)} \rightarrow \text{C}_2\text{H}_3 + \text{H}_2\text{O (H}_2\text{)} \qquad \text{(R7)}$$
$$\text{C}_2\text{H}_3 \text{ (+M)} \rightarrow \text{C}_2\text{H}_2 + \text{H (+M)} \qquad \text{(R8)}$$
$$\text{C}_2\text{H}_2 + \text{O} \rightarrow \text{HCCO} + \text{H.} \qquad \text{(R9)}$$

Nitric oxide is then converted to hydrogen cyanide by reaction with ketenyl,

$$HCCO + NO \rightarrow HCN + CO_2. \qquad (R1b)$$

The other product channel,

$$HCCO + NO \rightarrow HCNO + CO, \qquad (R1a)$$

is not effective as a nitric oxide removal step, because reactions of HCNO with O and OH recycle the HCNO back to NO,

$$HCNO + O \rightarrow HCO + NO \qquad (R2)$$

$$HCNO + OH \rightarrow HCOH + NO, \qquad (R3)$$

as discussed in the Introduction. When ethylene or acetylene is the reburn fuel, the route to ketenyl is even simpler - (R7), (R8), and (R9) for C_2H_4 and (R9) for C_2H_2.

The situation is a little more complicated when methane or natural gas is the reburn fuel. Somewhat surprisingly, the methyl radical primarily reacts with itself under the conditions of interest, even when the reactants are highly diluted with nitrogen, as in the experiments modeled by Glarborg, et al., i.e.

$$CH_3 + CH_3 (+M) \rightarrow C_2H_6 (+M) \qquad (R10)$$

$$CH_3 + CH_3 \rightarrow C_2H_5 + H. \qquad (R11)$$

The conversion of methyl to ethane and ethyl is even more dominant under the less dilute conditions studied by Prada and Miller. Nevertheless, the reaction of methyl with NO,

$$CH_3 + NO \rightarrow HCN + H_2O \qquad (R4a)$$

$$\rightarrow H_2CN + OH, \qquad (R4b)$$

followed by dissociation of H_2CN, makes a contribution to the NO → HCN conversion. The contribution is greater in the experiments considered by Glarborg, et al., because the smaller fuel concentrations allow $CH_3 + NO$ to compete more favorably with the methyl recombination reactions. Once ethane and ethyl are formed, the paths leading to ketenyl and NO conversion are the same as for the C_2 hydrocarbon fuels.

Obviously, the importance of the $CH_3 + NO$ reaction depends on the value of its rate coefficient. Miller, et al. [22] have recently studied this reaction theoretically using BAC-MP4 potential energy surface information. They obtained for k_4 the expression, $k_4 = 3.0 \times 10^{-1} T^{3.52} \exp(-3950/RT)$ cm^3/mole-sec., in the temperature range, 1000 K < T < 2500 K. This expression is in remarkably good agreement with the experimental results of Braun-Unkhoff, et al. [13] and Hennig and Wagner [23] and was used by Prada and Miller and Glarborg, et al. in their modeling. It yields rate coefficients that are substantially larger than those used in previous modeling, except for the work of Stapf and Leuckel, who used the Braun-Unkhoff, et al. expression directly.

The area of greatest uncertainty in the fuel oxidation mechanism is the fate of vinyl. Although the rate coefficient of the $C_2H_3 + O_2$ reaction appears to be reasonably well established, the product distribution for T > 1000 K is not [17, 18]. Potentially this could be important. In the present model the dominant channel is vinoxy + O, which can lead to ketenyl (and thus NO removal) through the sequence,

$$CH_2HCO + OH \rightarrow CH_2CO + H_2O \quad (R12)$$
$$CH_2CO + OH \rightarrow HCCO + H_2O, \quad (R13)$$

as shown in Fig. 1. In the modeling of Prada and Miller, it was necessary to suppress this and other paths to ketene initiated by $C_2H_3 + O_2$ in order to avoid overpredicting the NO removal. The $CH_2O + HCO$ product channel, known to be dominant at low temperature [24, 25], is benign in this regard.

The vinyl dissociation rate coefficient, which of course depends on temperature, pressure, and composition, has only recently been measured directly for the first time [26], and then only for a narrow range of conditions. Most of the usable information on the reaction is data for the reverse (addition) rate coefficient at low temperature. However, using these results requires knowledge of ΔH_f° for C_2H_3, which has been a source of controversy in the recent past [17, 26, 27].

It should be cautioned that the mechanism discussed here is strictly valid only under "radical-poor" conditions such as those normally encountered in a plug-flow reactor for 1000 K $< T <$ 1400 K. For "radical-rich" situations, e.g. in a low-pressure flame [8] or stirred reactor [7], methyl and ketenyl are more likely to be converted to smaller hydrocarbon radicals, e.g.

$$CH_3 + OH \rightarrow {}^1CH_2 + H_2O \quad (R14)$$
$$HCCO + H \rightarrow {}^1CH_2 + CO, \quad (R15)$$

followed by ${}^1CH_2 \rightarrow {}^3CH_2 \rightarrow CH \rightarrow C$. Under such conditions the dominant NO removal steps normally will be [6, 7, 8]

$$C + NO \rightarrow CN + O$$
$$\text{and} \quad CH + NO \rightarrow HCN + O. \quad (R17)$$

III. The Reactions of HCNO with O and OH

In this section we consider the fate of HCNO once it is formed as a product in reaction (R1a). More precisely, we want to estimate rate coefficients for the reactions,

$$HCNO + O \rightarrow HCO + NO \quad (R2)$$
$$\text{and} \quad HCNO + OH \rightarrow HCOH + NO. \quad (R3)$$

Both reactions (R2) and (R3) are exothermic, $\Delta H^\circ \approx$ -66 kcal/mole for reaction (R2) and $\Delta H^\circ \approx$ -3 kcal/mole for (R3), and both take place over relatively deep potential wells, roughly 83 kcal/mole for (R2) and 50 kcal/mole for (R3). Therefore, there is reason to believe that both k_2 and k_3 should be determined by the rate of addition of the radicals to HCNO and that these processes should have relatively low energy barriers. However, since HCNO is a singlet, it is not obvious *a priori* that the barriers are zero. Nevertheless, extensive searches at the G2Q level [28] of electronic structure theory convinced us that neither reaction had a barrier.

In order to make estimates of k_2 and k_3, we have used the "maximum free energy" method of Quack and Troe [29], which is very simple to implement, requiring only information about the "endpoints" of the reaction, i.e. the stable reactants and the product. The method uses empirical interpolation formulas to obtain values of the Gibbs free energy along the reaction path

between these endpoints. The maximum value obtained determines the rate coefficient, equivalent in principle to canonical variational transition-state theory. The properties of the stable species required for the calculation were determined from electronic structure theory - geometries were obtained using MP2 (Möller-Plessett second-order perturbation theory), energies came from G2 calculations, and the vibrational frequencies used were obtained by scaling Hartree-Fock frequencies.

The rate coefficients obtained are plotted in Fig. 2. In both cases the calculations indicate that the rate coefficient increases slightly with temperature. However, barrierless reactions normally have rate coefficients that decrease or remain relatively constant with T, and we believe that the present increase may simply be an artifact of the calculation procedure. Consequently, we interpret these results as indicating that $k_2 \approx 7 \times 10^{13}$ cm^3/mole-sec. and $k_3 \approx 2 \times 10^{13}$ cm^3/mole-sec independent of temperature (shown as the solid line in Fig. 2). These rate coefficients are approximately a factor of 2 to 3 smaller than those used in the modeling of Glarborg, et al. and Prada and Miller, but they are sufficiently large to insure that the primary fate of HCNO is to regenerate nitric oxide.

Initially, we expected the principal products of reaction (R3) to be CH_2O (formaldehyde) + NO. Such products could be formed from a 1, 2 hydrogen shift in the initial adduct. However, somewhat surprisingly, G2Q calculations show that the saddle point corresponding to this 1, 2 hydrogen transfer lies 13 kcal/mole higher in energy than the HCNO + OH reactants, effectively shutting off this product channel.

IV. The Reaction Between Ketenyl and Nitric Oxide

The reaction between HCCO and NO is clearly the most important reaction for reburning under flow reactor conditions, at least given our present knowledge of the fuel oxidation chemistry. Because the reactions of HCNO with O and OH are very fast and form NO as a product, the extent to which HCCO + NO forms stable HCN and CO_2 is critical. Reaction (R1) actually has three energetically accessible channels [30],

$$\begin{aligned} HCCO + NO &\rightarrow HCNO + CO && \text{(R1a)} \\ &\rightarrow HCN + CO_2 && \text{(R1b)} \\ &\rightarrow HONC + CO, && \text{(R1c)} \end{aligned}$$

under combustion conditions. We want to determine $\alpha(T)$ and $\beta(T)$, where

$$\alpha(T) = k_{1b}(T)/k_1(T)$$

and

$$\beta(T) = k_{1c}(T)/k_1(T).$$

Figure 3 is a reaction coordinate diagram taken from the work of Nguyen et al. [30], who characterized the reaction paths from QCISD and MP4 electronic structure calculations. To calculate $\alpha(T)$ and $\beta(T)$ we have supplemented their calculations with our own computations of structures and vibrational frequencies of the intermediate saddle points using density functional theory (DFT) [31, 32], with several different functionals [31], and MP2. With a couple of minor exceptions, all these methods give essentially the same results. We actually use in our

calculations of $\alpha(T)$ and $\beta(T)$ the frequencies and moments of inertia from the electronic structure calculations using the b3pw91 functional [31].

There are two paths leading from reactants to the initial adducts (or complexes) marked (x) and (y) in Fig. 3, neither of which has a potential energy barrier. Such processes should be treated using variational transition state theory. However, we do not have enough information about the potential at our disposal to do such a calculation, and this part of the process has relatively little effect on $\alpha(T)$ anyway, since the subsequent barriers to rearrangement for the major product channels lie well below the reactants on the potential energy surface. In such cases, the initial transition-state dividing surfaces, TSDS-0 and TSDS-1 of Fig. 3, normally determine the total rate coefficient and the subsequent rearrangements determine the product distribution [33]. However, at sufficiently high temperatures there is always the possibility of the initial complexes redissociating back to reactants. This process is also governed by TSDS-0 and TSDS-1. To account accurately for this possibility, we have adjusted the properties of TSDS-0 and TSDS-1 as a function of temperature, mimicking the results of a variational transition state theory calculation, to give the experimental value of the total rate coefficient, $k_1 = k_{1a} + k_{1b} + k_{1c}$.

Figure 4 shows all the experimental data to date on $k_1(T)$. Although Boullart, et al. [16] report a rate expression for k_1 that increases with temperature, their data is quite consistent with a constant value of $k_1 = 2.4 \times 10^{13}$ cm^3/mole-sec, as shown in Fig. 4. Because of this and because we do not expect k_1 to increase with T, we have varied the properties of TSDS-0 and TSDS-1 (assuming them to be the same for simplicity) to give this value of k_1 (normally $k_1 = 2.4 \pm 0.1$ cm^3/mole-sec.) at all temperatures considered, $300\ K < T < 2000\ K$.

Using methods introduced by Miller, Parrish, and Brown [34], we treat all the possible rearrangements of the collision complex as a stochastic process, allowing for passage back and forth between the various configurations shown in Fig. 4 any number of times. Because the lifetimes of the intermediate complexes are very short, the reaction occurs without collisions. Thus total energy E and total angular momentum must be conserved explicitly in the calculations. We can write rate coefficient expressions for the three product channels as follows:

$$k_{1a}(T) = [hQ_R(T)g_e(T)]^{-1}\sum_J (2J+1)\int_0^\infty \frac{f_5 F_z}{D}\left\{f_0 f_2 F_w + f_1 (F_w F_x - f_3^2)\right\}\exp(-E/k_BT)\,dE \qquad (1)$$

$$k_{1b}(T) = [hQ_R(T)g_e(T)]^{-1}\sum_J (2J+1)\int_0^\infty \frac{f_4 f_6}{D}\left\{f_0 f_2 F_w + f_1 (F_w F_x - f_3^2)\right\}\exp(-E/k_BT)\,dE \qquad (2)$$

$$k_{1c}(T) = [hQ_R(T)g_e(T)]^{-1}\sum_J (2J+1)\int_0^\infty \frac{f_3 f_7}{D}\left\{f_0 (F_y F_z - f_4^2) + f_1 f_2 F_z)\right\}\exp(-E/k_BT)\,dE \qquad (3)$$

where $$D(E, J) = (f_3^2 - F_w F_x)(f_4^2 - F_y F_z) - f_2^2 F_w F_z, \quad (4)$$

$$F_x(E, J) = f_0 + f_2 + f_3, \quad (5)$$

$$F_y(E, J) = f_1 + f_2 + f_4 + f_5, \quad (6)$$

$$F_z(E, J) = f_4 + f_6, \quad (7)$$

and $$F_w(E, J) = f_3 + f_7. \quad (8)$$

In these expressions k_B is Boltzmann's constant, h is Planck's constant, T is the temperature, J is the total angular momentum quantum number, and Q_R (T) is the vibrational-rotational-translational partition function of the reactants (not including electronic or center-of-mass contributions). The function $g_e(T)$ is the electronic partition function of the reactants,

$$g_e(T) = 2[2 + 2\exp(-346/RT)]. \quad (9)$$

The functions $f_i(E, J)/h$, i = 0, 1, ..., 7, represent microcanonical/fixed-J probability fluxes per unit energy through the indicated transition-state dividing surfaces of Fig. 3. They are the same in both directions because of microscopic reversiblity. For purely classical reaction-path motion, f_i (E, J) is the sum of states with total angular momentum quantum number equal to J and energy less than or equal to E. The f_i (E, J)'s (i = 2, ... 7) are evaluated exactly [34, 22, 33] in the harmonic-oscillator/rigid-rotor approximation with the potential along the reaction coordinate assumed to be described by the Eckart function. Our method of evaluating integrals such as (1), (2), and (3) is described in previous papers [34, 22, 33].

The results for $k_1(T)$, $\alpha(T)$, and $\beta(T)$ are given in Table 1. The branching fraction $\alpha(T)$ decays from about 0.8 at 300 K to 0.3 at 2000 K; $\beta(T)$ increases with temperature, but never gets as large as 10^{-2}. Reaction (R1c) thus can safely be neglected for most situations of interest.

The theoretical values of $\alpha(T)$, along with the experimental result of Boullart, et al. [16] and the value used in our modeling, are plotted in Fig. 5. Theoretically, $\alpha(T)$ is represented quite accurately by the exponential function,

$$\alpha(T) = 0.985\exp(-T/1748), \quad (10)$$

shown as the dashed line in Fig. 5. Using $k_1 = 2.4 \times 10^{13}$ cm^3/mole-sec., the individual rate coefficients for (R1a) and (R1b) can be expressed in the modified Arrhenius form as

$$k_{1a} = 1.17 \times 10^{13}\, T^{0.65} \text{ cm}^3\text{/mole-sec.} \quad (11)$$

and $$k_{1b} = 1.45 \times 10^{16}\, T^{-0.969}\exp(-648/RT) \text{ cm}^3\text{/mole-sec.} \quad (12)$$

The theoretical result for $\alpha(T)$ is substantially larger than that obtained experimentally by Boullart, et al. [16], as shown in Fig. 5, but it is only slightly smaller than the value used in the two modeling studies [17, 18]. The theoretical and modeling values can probably be made consistent with relatively minor modifications to both. However, the difference between the theoretical and experimental results is much too large to be accounted for by small errors in the theoretical parameters. Nguyen, et al. [30] have suggested that other reaction paths to CO (the species measured by Boullart, et al. were CO and CO_2) might exist, which could explain the difference between theory and experiment. However, they were not able to find such low-

energy paths; we also have not been able to find them. Consequently, we must conclude that there simply is a large discrepancy between the best experiment and the best theory for $\alpha(T)$.

Concluding Remarks

The present investigation was undertaken to obtain theoretical values for some critical kinetic parameters identified in modeling NO_x reburning experiments under flow-reactor conditions. Specifically, using PES information from a variety of sources, we have calculated rate coefficients for the reactions,

$$HCNO + O \rightarrow HCO + NO \qquad (R2)$$

and

$$HCNO + OH \rightarrow HCOH + NO, \qquad (R3)$$

and conclude that $k_2 \approx 7 \times 10^{13}$ cm^3/mole-sec and $k_3 \approx 2 \times 10^{13}$ cm^3/mole-sec independent of temperature for 300 K < T < 2700K. With such fast reactions converting HCNO back to NO, reaction (R1a),

$$HCCO + NO \rightarrow HCNO + CO, \qquad (R1a)$$

is not effective in the NO → HCN conversion. Thus the branching fraction of (R1), $\alpha(T)$, becomes an important parameter in the model,

$$HCCO + NO \rightarrow HCNO + CO \qquad (R1a)$$

$$\rightarrow HCN + CO_2, \qquad (R1b)$$

where $\alpha(T) = k_{1b}(T)/k_1(T)$.

Again using PES information from a variety of sources, we have utilized statistical-theoretical methods to calculate $\alpha(T)$,

$$\alpha(T) = 0.985 \exp(-T/1748),$$

for 300 K < T < 1000 K. This result is probably compatible with the value of $\alpha(T) \approx 0.65$, independent of temperature, used in the modeling of Glarborg, et al. [17] and Miller and Prada [18]. However, it is inconsistent with $\alpha = 0.23$ at T = 700 K, the value obtained experimentally by Boullart, et al. [16]. The origin of the discrepancy is not apparent.

Using $k_1 = 2.4 \times 10^{13}$ cm^3/mole-sec independent of temperature, k_{1a} and k_{1b} can be expressed as

$$k_{1a} = 1.17 \times 10^{13}\, T^{0.65} \text{ cm}^3\text{/mole-sec}$$

and

$$k_{1b} = 1.45 \times 10^{16}\, T^{-0.968} \exp(-648/RT) \text{ cm}^3\text{/mole-sec},$$

for 300 K < T < 2000 K. We recommend using these values in future modeling.

Acknowledgements

This work was supported by the United States Department of Energy, Office of Basic Energy Sciences, Division of Chemical Sciences and by the CHEC Research Program. The research program CHEC (Combustion and Harmful Emission Control) is co-funded by the Danish Technical Research Council, Elsam (The Jutland - Funen Electricity Consortium), Elkraft (The Zealand Electricity Consortium), and the Danish Ministry of Energy.

References

1. Wendt, J. O. L., Sterling, C. V., and Matovich, M. A., *Fourteenth Symposium (International) on Combustion*, The Combustion Institute, Pittsburgh, PA, 1973, p. 897.

2. Bilbao, R., Alzueta, M. U., and Millera, A., *Ind. Eng. Chem. Res.* **34**: 4531 (1995) and references cited therein

3. Kolb, T., Jansohn, P., and Leuckel, N., *Twenty-Second Symposium (International) on Combustion*, The Combustion Institute, Pittsburgh, PA 1989, p. 1193

4. Rota, R., Bonini, F., Servida, A., Norbidelli, M., and Carrá, S., *Combust. Sci. and Tech.* **123**: 83-105 (1997)

5. Kilpinen, P., Glarborg, P., and Hupa, M., *Ind. Eng. Chem. Res.* **31:** 1477 (1992)

6. Miller, J. A. and Bowman, C.T., *Progress in Energy and Combustion Science* **15**: 287-338 (1989)

7. Glarborg, P., Miller, J. A. and Kee, R. J., *Combust. Flame* **65**: 177 (1986)

8. Thorne, L. R. Branch, M. C., Chandler, D. W., Kee, R. J., and Miller, J. A., *Twenty-First Symposium (International) on Combustion*, Pittsburgh, PA, 1988, p. 965

9. Stapf, D. and Leuckel, W., *Twenty-Sixth Symposium (International) on Combustion*, The Combustion Institute, Pittsburgh, PA, 1996, pp. 2083-2090

10. Nishioka, M., Kondoh, Y., and Takeno, T., *Twenty-Sixth Symposium (International) on Combustion*, The Combustion Institute, Pittsburgh, PA, 1996, pp. 2139-2145

11. Glarborg, P. and Hadvig, S., "Development and Test of a Kinetic Model for Natural Gas Combustion," Nordic Gas Technology Center, DK, ISBN 87-89309-44-8 (1991)

12. Bockhorn, H., Chevalier, Ch., Warnatz, J., and Weyrauch, V., VDI-Berichte **922**: 171 (1991)

13. Braun-Unkhoff, M., Naumann, C., Wintergerst, K., and Frank, P., *UDI-Berichte* **1090**: 287-294 (1993)

14. Unfried, K. G., Glass, G. P., and Curl, R. F., *Chem. Phys. Lett.* **177**: 33-38 (1991)

15. Temps, F., Wagner, H. Gg., and Wolf, M., *Z. Phys. Chem.* **176**: 27-39 (1992)

16. Boullart, W., Nguyen, M. T., and Peeters, J., *J. Phys. Chem.* **98**: 8036-8043 (1994)

17. Glarborg, P., Alzueta, M. U., Dam-Johansen, K., and Miller, J. A., "Kinetic Modeling of Hydrocarbon/Nitric Oxide Interactions in a Flow Reactor," *Combust. Flame*, in press (1998)

18. Prada, L. and Miller, J. A., "Reburning Using Several Hydrocarbon Fuels: A Kinetic Modeling Study," *Comb. Sci. Tech.*, in press (1998)

19. Cooper, W. F., Park, J., and Hershberger, J. F., *J. Phys. Chem.* **97**: 3238 (1993)

20. Lin, M. C., He, Y., and Melius, C. F., *J. Phys. Chem.* **97**: 9124 (1993)

21. Miller, J. A., *Twenty-Sixth Symposium (International) on Combustion*, The Combustion Institute, Pittsburgh, PA, 1996, pp. 461-480

22. Miller, J.A., Melius, C. F., and Glarborg, P., "The CH_3 + NO Rate Coefficient at High Temperatures: Theoretical Analysis and Comparison with Experiment," *Int. J. Chem. Kin.*, in press (1997)

23. Hennig, G. and Wagner, H. Gg., *Ber Bunsenges. Phys. Chem.* **98**: 749 (1994)

24. Slagle, I. R., Park, J.-Y., Heaven, M. C., and Gutman, D., *J. Am. Chem. Soc.* **106**: 4356-4361 (1984)

25. Knyazev, V. D., and Slagle, I. R., *J. Phys. Chem.* **99**: 2247-2249 (1995)

26. Knyazev, V. D. and Slagle, I. R., *J. Phys. Chem* **100**: 16899-16911 (1996)

27. Kaiser, E. W. and Wallington, T. J., *J. Phys. Chem.* **100**: 4111-4119 (1996)

28. Durant, J. L., and Rohlfing, C. M., *J. Chem. Phys.* **98**: 8031 (1993)

29. Quack, M. and Troe, J., *Ber. Bunsenges. Phys. Chem.* **81:** 329-337 (1977)

30. Nguyen, M. T., Boullart, W., and Peeters, J., *J. Phys. Chem.* **98**: 8030-8035 (1994)

31. Durant, J. L., "Computational Thermochemistry and Transition States," to appear in *Computational Thermochemistry* (K. Irikura and D. Frurip, Eds.)

32. Durant, J. L., *Chem. Phys. Lett.* **256**: 595-602 (1996)

33. Miller, J. A. and Melius, C. F., *Twenty-Fourth Symposium (International) on Combustion*, The Combustion Institute, Pittsburgh, PA, 1992, pp. 719-726

34. Miller, J. A., Parrish, C., and Brown, N. J., *J. Phys. Chem.* **90**: 3339 (1986)

Figure and Table Captions
Figures

1. Reaction path diagram for NO reburning under flow-reactor conditions.

2. Theoretical predictions of rate coefficients for reactions (R2), HCNO + O → HCO + NO and (R3) HCNO + OH → HCOH + NO. The points are the results of the maximum free energy calculations and the solid lines are our recommendations for use in modeling, $k_2 = 7 \times 10^{13}$ cm^3/mole-sec. and $k_3 = 2 \times 10^{13}$ cm^3/mole-sec.

3. Potential energy diagram for the HCCO + NO → products reaction. The numbers identify transition-state dividing surfaces used in the statistical calculations. The letters denote complexes with the chemical structure shown. The potential energies were taken from Nguyen, et al. [30].

4. The total rate coefficient $k_1(T)$ for reaction (R1), HCCO + NO → Products. The experimental points are from Boullart, et al. [16], Unfried, et al. [14], and Temps, et al. [15]. The solid line, $k_1 = 2.4 \times 10^{13}$ cm^3/mole-sec., is our recommendation for use in modeling. The results for k_{1a} and k_{1b} given in the text are based on this total rate coefficient.

5. The branching fraction $\alpha(T)$ of the HCCO + NO → Products reaction, where $\alpha(T) = k_{1b}(T)/k_1(T)$, i.e. the fraction that produces HCN + CO_2. The triangles indicate the value of α used in the modeling of Glarborg, et al. [7] and Prada and Miller [18]. The experimental point is due to Boullart, et al [16]. The dashed line is a least-squares fit to the theoretical calculations, $\alpha(T) = 0.985 \exp(-T/1748)$. The branching fraction can also be represented reasonably well by the Arrhenius expression, $\alpha(T) = 342\ T^{-0.896} \exp(-522/RT)$.

Tables

1. Results from the statistical-theoretical calculations. $\alpha(T) = k_{1b}(T)/k_1(T)$ and $\beta(T) = k_{1c}(T)/k_1(T)$. The properties of TSDS-0 and TSDS-1 were adjusted to give a value of $k_1 \approx 2.4 \times 10^{13}$ cm^3/mole-sec.

Table I

Theoretical Results

T (K)	k_1 (cm^3/mole-sec.))	$\alpha(T)$	$\beta(T)$
300	2.26×10^{13}	0.803	3.62×10^{-6}
500	2.30×10^{13}	0.743	2.27×10^{-5}
600	2.43×10^{13}	0.710	4.73×10^{-5}
700	2.32×10^{13}	0.676	8.97×10^{-5}
900	2.44×10^{13}	0.603	2.61×10^{-4}
1000	2.38×10^{13}	0.566	4.11×10^{-4}
1200	2.30×10^{13}	0.500	8.78×10^{-4}
1500	2.36×10^{13}	0.418	2.05×10^{-3}
1700	2.31×10^{13}	0.368	3.29×10^{-3}
2000	2.36×10^{13}	0.307	5.85×10^{-3}

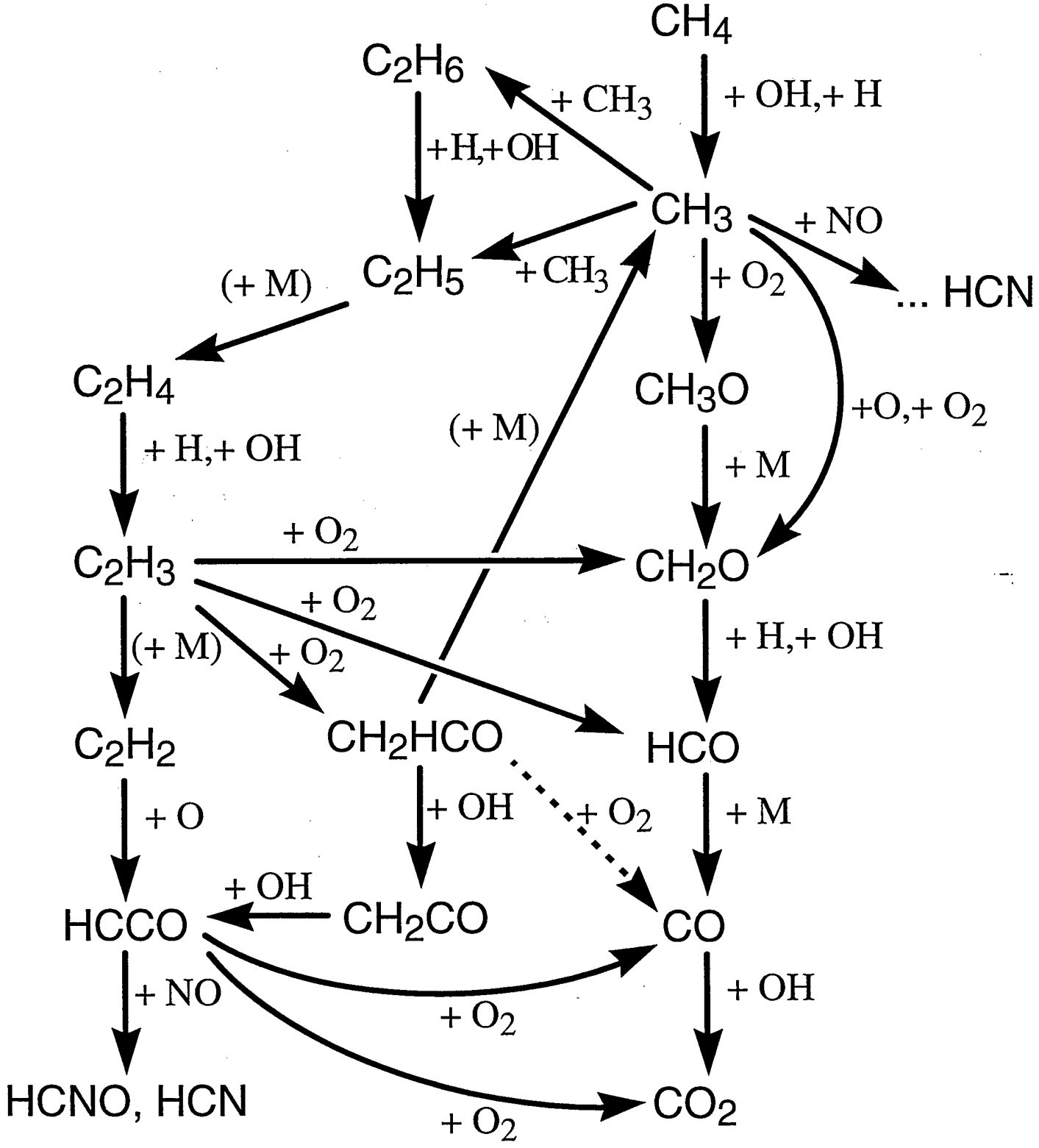
CH4
C2H6
+ CH3
+ OH,+ H
+H,+OH
CH3
+ NO
C2H5
+ CH3
+ O2
... HCN
(+ M)
C2H4
CH3O
+O,+ O2
+ H,+ OH
(+ M)
+ M
+ O2
C2H3
CH2O
+ O2
+ H,+ OH
(+ M)
+ O2
C2H2
CH2HCO
HCO
+ O
+ OH
+ O2
+ M
+ OH
HCCO
CH2CO
CO
+ NO
+ O2
+ OH
HCNO, HCN
+ O2
CO2

Fig. 1

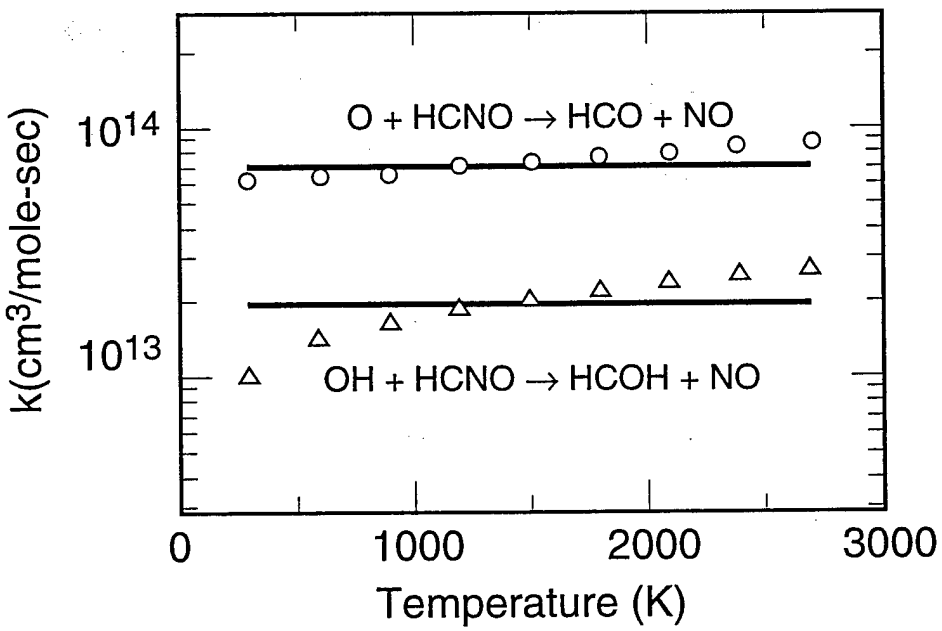
k(cm3/mole-sec)
10^14
10^13
O + HCNO → HCO + NO
OH + HCNO → HCOH + NO
0
1000
2000
3000
Temperature (K)

Fig. 2

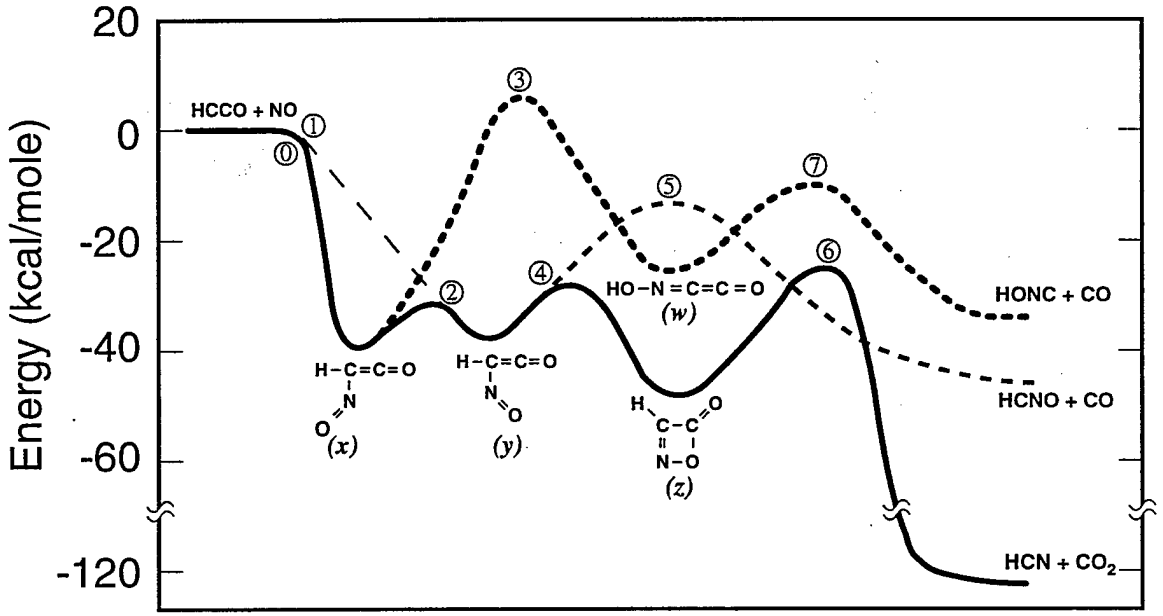
20
0
-20
-40
-60
-120
Energy (kcal/mole)
HCCO + NO
0
1
2
3
4
5
6
7
HO–N=C=C=O
(w)
H–C=C=O
N
O
(x)
H–C=C=O
N
O
(y)
H
C–C
N–O
(z)
HONC + CO
HCNO + CO
HCN + CO2

Fig. 3

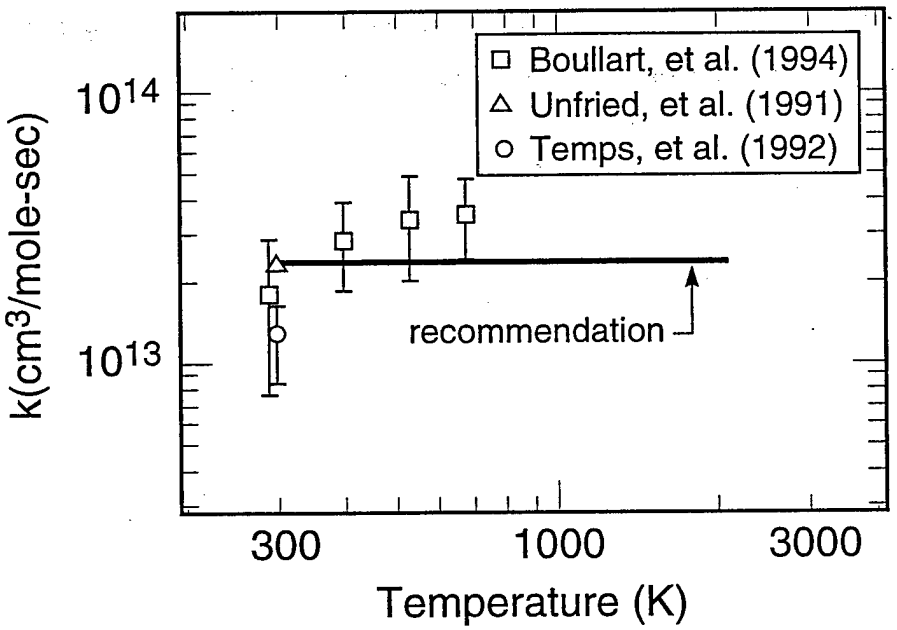
Boullart, et al. (1994)
Unfried, et al. (1991)
Temps, et al. (1992)
recommendation
10^{14}
10^{13}
k(cm³/mole-sec)
300
1000
3000
Temperature (K)

Fig. 4

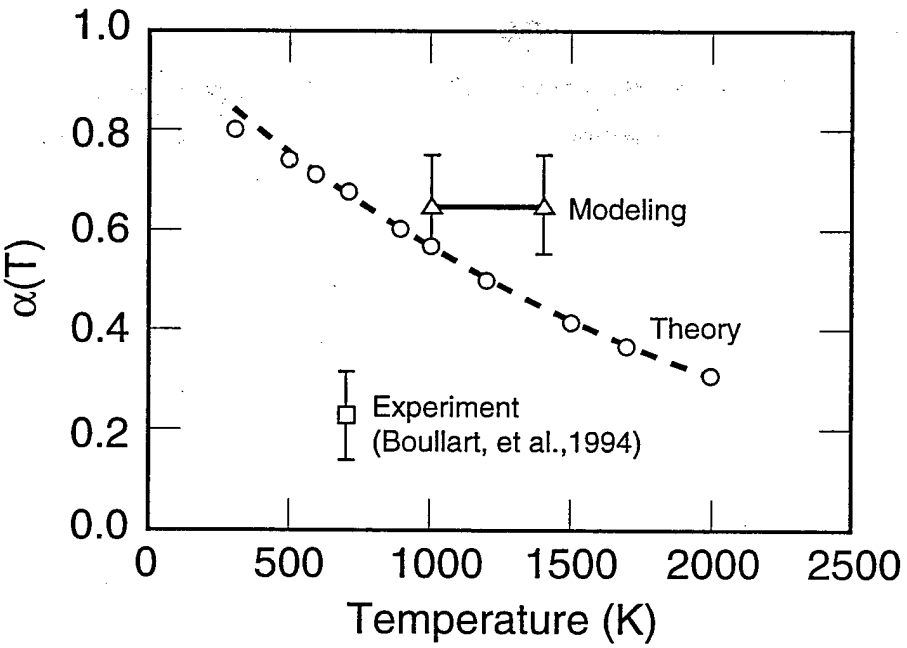
1.0
0.8
0.6
0.4
0.2
0.0
α(T)
0
500
1000
1500
2000
2500
Temperature (K)
Modeling
Theory
Experiment
(Boullart, et al.,1994)

Fig. 5

Report Number (14) SAND--98-8450C
CONF-980804--

Publ. Date (11) 199808
Sponsor Code (18) DOE/EE, XF
UC Category (19) UC-1409, DOE/ER

DOE